Polymer Science, Ser. A, Vol. 40, No. 12, 1998, pp. 1259–1267. Translated from Vysokomolekulyarnye Soedineniya, Ser. A, Vol. 40, No. 12, 1998, pp. 2029–2039.

Dynamics of Paramagnetic Charge Carriers in Poly(tetrathiafulvalene)[1]

V. I. Krinichnyii*, N. N. Denisov*, H.-K. Roth, E. Fanghänel***, and K. Lüders******

* *Institute of Chemical Physics Research, Russian Academy of Sciences, Chernogolovka, Moscow oblast, 142432 Russia*

** *Thuringisches Institut für Textil- and Kunstoff-Forschung e.V. (TITK), Breitscheidstrasse 97, Rudolstadt-Schwasza, D-07407 Deutschland*

*** *Martin-Luther-Universität Halle, Geusaer Strasse, Merseburg, D-06217 Deutschland*

**** *Hochschule für Technik, Wirtschaft und Kultur, PF 66 Leipzig, D-04251 Deutschland*

Received March 16, 1998;
Revised Manuscript Received July 8, 1998

Abstract—Magnetic-relaxation parameters of the paramagnetic centers in poly(tetrathiafulvalene) samples with different doping levels were studied by 2-mm-band EPR spectrometry. Electron relaxation time and the rates of intra- and interchain spin diffusion rates were separately determined by the steady-state saturation technique. Anisotropic superslow librations of polymer chains were measured by the saturation transfer technique. The intensity and the activation energy of these librations were found to depend on the sample doping level. The initial polymer features isoenergetic charge transfer by small polarons in agreement with the Kivelson theory. The interchain mobility of the molecular-lattice polarons in doped samples is correlated with the libration motions and is described with good precision within the framework of the variable-range hopping charge transfer mechanism.

INTRODUCTION

In recent years, considerable attention of researchers has been drawn to the study of the charge transfer mechanisms in quasi-one- dimensional semiconductors [1–3]. Doping of these compounds with different counterions leads to an increase in their conductivity by several orders of magnitude, which is accompanied by an increase in dimensionality of the organic semiconductors and a change in the charge transfer mechanism. For example, the doping of *trans*-poly(acetylene) with iodine increases the specific conductivity by a factor of 10^{10}–10^{12} [4]. The mechanism of charge transfer in this organic semiconductor changes from the isoenergetic tunneling (described within the framework of the Kivelson theory) to the activation transfer and then to the variable-range hopping charge transfer (within the framework of the Mott theory) [5].

It is commonly accepted [6] that charge transfer in most of the π-conjugated polymers is mediated by nonlinear excitations, called polarons, and characterized by two intrinsic energy levels in the forbidden band. A polaron possesses, in addition to the unit charge, an uncompensated spin that makes EPR spectroscopy an effective tool for the investigation of relaxation and electron-dynamic properties of organic polymeric semiconductors [7, 8]. These investigations are conventionally performed by measuring the centimeter- and meter-band EPR spectra at a comparatively weak magnetic field strength ($B_0 \leq 0.33$ T), in which the signal components from organic free radicals are poorly resolved. Moreover, the rate of cross relaxation between individual spin packets in these wavebands may exceed the effective EPR signal linewidth of the sample, thus reducing sensitivity of this method with respect to the charge and spin dynamics.

Poly(tetrathiafulvalene) (PTTF) has a chain structure in which the TTF monomer units are linked by phenyl or tetrahydroanthracene bridges (Fig. 1). This polymer offers a convenient model system for the investigation of spin and charge dynamics in organic polymeric semiconductors. The EPR measurements of some PTTF samples in a 3-cm band [9, 10] showed that the spectra represent a superposition of asymmetric and symmetric signals, which were attributed to localized and mobile paramagnetic centers, respectively. It was found that the relative contents of these centers depend on the doping level and structure of the sample.

Previously, we have demonstrated that EPR spectroscopy in the 2-mm waveband provides the most complete and correct information on the nature and dynamics of paramagnetic centers in various conju-

[1] This work was partly supported by the Russian Foundation for Basic Research, projects nos. 97-03-33707 and 96-03-33755.

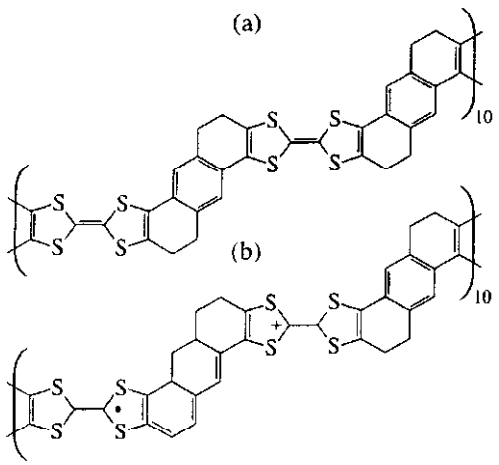

Fig. 1. Molecular structure of (a) the initial PTTF sample and (b) a iodine doped structure with polaron in the chain. Note that the actual polaron length is greater than that depicted in this schematic diagram.

gated polymers [11–13], including PTTF with monomer units linked by phenyl bridges [14, 15]. A high spectral resolution achieved by measurements in this spectral band and the appearance of some special effects in high fields ($B_0 \approx 5$ T) provide the possibility of separately determining the spin–lattice (T_1) and spin–spin (T_2) relaxation times and measuring the mobility of polaron charge carriers both along the macromolecular chain and between macromolecules. Moreover, EPR measurements using the SHF saturation transfer technique allow us to study superslow small-scale vibrations of the polymer chains with localized polarons.

Below we present the results of (mostly) 2-mm-band EPR investigations of the spin and molecular dynamics in both undoped (initial) and doped samples of PTTF with the monomer units linked by tetrahydroanthracene bridges.

EXPERIMENTAL

The samples of powdered PTTF with different doping levels $y = [I]/[TTF] = 0$ (PTTF-1), 0.08 (PTTF-2), and 0.12 (PTTF-3) were synthesized by the method described elsewhere [16]. The degrees of polymerization and the levels of doping were determined by elemental analyses. The EPR measurements were conducted using 3-cm (PS100.X) and 2-mm waveband ranges, the latter variant being previously described in [11, 17, 18]. The exact phase adjustment of the SHF and the HF modulation oscillations was performed using a lateral single-crystal standard (dibenzotetrathiafulvelene) $^{+}PtBr_6^{-}$ using a procedure described in [11, 18]. The same standard was used for determining the relative content of paramagnetic centers. Another standard (Mn^{2+} with $g_{eff} = 2.00102$ and $a_{eff} = 8.74$ mT) was used for calibration of the g tensor components and the constant magnetic field sweep scale in the 2-mm waveband. The relaxation parameters in the 2-mm waveband were studied by monitoring both the imaginary and real parts of the magnetic susceptibility.

RESULTS AND DISCUSSION

The 3-cm EPR spectrum of PTTF samples contains a nearly symmetric signal with $g_{iso} = 2.0065$ and the peak separation $\Delta B_{pp} = 0.27$ mT (PTTF-1) and 0.63 mT (PTTF-2 and PTTF-3). Assuming that the initial sample contains predominantly localized paramagnetic centers, we may estimate the minimum number of protons H on which the unpaired electron is localized using the formula [19]

$$\Delta B_{pp} = \frac{Q}{\sqrt{2N}}, \quad (1)$$

where Q is the Mac-Connell constant. Adopting the value $Q = 2.25$ mT for the benzene anion radical, we obtain $N \approx 35$. Because each monomer unit contains six protons, we may conclude that the delocalization length of paramagnetic centers in the polymer equals approximately six monomer units. This value is close to the degree of polymerization determined by the data of elemental analyses [10].

In the doped PTTF samples, the concentration of paramagnetic centers exhibits a growth by a few percent in the temperature range 90–300 K, increasing from 3.1×10^{18} spin/g in PTTF-1 to 3.9×10^{18} in PTTF-2 and then to 4.1×10^{18} in PTTF-3. Thus, the EPR line broadening upon doping of the polymer is caused by increasing spin–spin or spin–lattice coupling as a result of growing mobility of a part of the spin centers.

Figure 2c shows the absorption EPR spectra of the samples measured in the 2-mm waveband. The results of computer simulation showed that PTTF contains the paramagnetic centers of two types with temperature-independent g tensor components: R_1 with $g_{xx} = 2.01292$, $g_{yy} = 2.00620$, $g_{zz} = 2.00251$ (Fig. 2a), and R_2 with $g_{\parallel} = 2.00961$, $g_{\perp} = 2.00585$ components of the R_1 radical are close to the values reported for the TTF radical cation [21], we may conclude that the x-, y, and z-axes of spin delocalization in the polymer are oriented along the crystallographic c-, b-, and a-axes of its macromolecules. The isotropic g values of the R_1 and R_2 radicals in PTTF are approximately equal: $\frac{1}{3}(g_{xx} + g_{yy} + g_{zz}) \cong \frac{1}{3}(g_{\parallel} + 2g_{\perp})$, which implies that the polymer contains immobile polarons (R_1), localized in the vicinity of structural defects, on the oxygen traps, or on the

short polymer chains, and mobile polarons (R_2), diffusing along the polymer chains at a minimum rate given by the formula [22]

$$\nu_{1D}^0 \geq (g_{xx} - g_e)\mu_B \hbar^{-1} B_0, \quad (2)$$

where $g_e = 2.00232$ is the g value of the free electron, μ_B is the Bohr magneton, $\hbar$ is the Planck constant, and B_0 is the applied magnetic field strength. In particular, for PTTF $\nu_{1D}^0 \geq 2 \times 10^9$ s^{-1}.

The high spectral resolution ensured by the 2-mm waveband EPR measurements allowed us to determine the ratios of the R_1 and R_2 radical concentrations (n_1/n_2, in spin/monomer). In the PTTF samples studied, these ratio were as follows: $1.3 \times 10^{-3}/4.3 \times 10^{-4}$ (PTTF-1), $1.1 \times 10^{-4}/2.1 \times 10^{-3}$ (PTTF-2), and $4.5 \times 10^{-5}/2.3 \times 10^{-3}$ (PTTF-3), and remained virtually constant in the entire temperature range 90–300 K.

As the temperature increases in this range, the signal width in the EPR spectrum of the initial sample decreases from 4.7 to 3.4 mT. At the same time, the EPR linewidth in the spectra of doped samples is almost independent of the temperature and amounts to 9.2 mT. The dopant-induced broadening of the EPR signal can be explained by a growth in the number of mobile charge carriers in PTTF, which is accompanied by increase in their interaction with other nonlinear excitations and with the lattice.

An increase in the magnetic field strength leads to a considerable decrease in the rate of exchange ν_{ex} between individual spin packets [23]. As a result, the EPR signals in the spectra of the samples studied exhibit broadening (similar to that observed in the samples of PTTF with the monomer units linked by phenyl bridges) beginning with $B_0 \approx 5$ T according to the law $\delta(\Delta B_{pp}) \sim \Delta\omega_{ij}^2/\nu_{ex}$ [24], where $\Delta\omega_{ij}$ is the separation of spin packets expressed in the frequency units. In strong fields, the exchange rate ν_{ex} decreases and the probability of saturation of the spin packet increases ($\gamma_e^2 B_1^2 T_1 T_2 > 1$, where γ_e is the gyromagnetic ratio for electron and B_1 is the magnetic component of the SHF polarization field). As a result, the EPR spectra of PTTF show manifestations of the rapid passage effects (Fig. 3). Because the shapes of the signals observed in the spectra of PTTF-2 and PTTF-3 differ very slightly, below we will discuss only the spectrum of the latter sample.

In the general case, an equation for the first derivative of the dispersion signal U can be written in the following form [25]:

$$U = u_1 \sin(\omega_m t) + u_2 \sin(\omega_m t \pm \pi) + u_3 \sin(\omega_m t - \pi/2), \quad (3)$$

where ω_m is the HF modulation frequency. Since the initial and doped PTTF samples obey the conditions

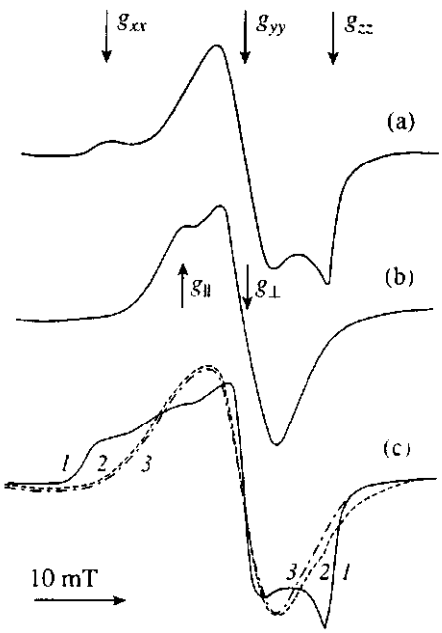

Fig. 2. The 2-mm waveband EPR absorption spectra (a, b) calculated for the in-phase components of the paramagnetic centers R_1 and R_2, respectively, and (c) experimentally measures in (*1*) PTTF-1, (*2*) PTTF-2, and (*3*) PTTF-3 samples at room temperature.

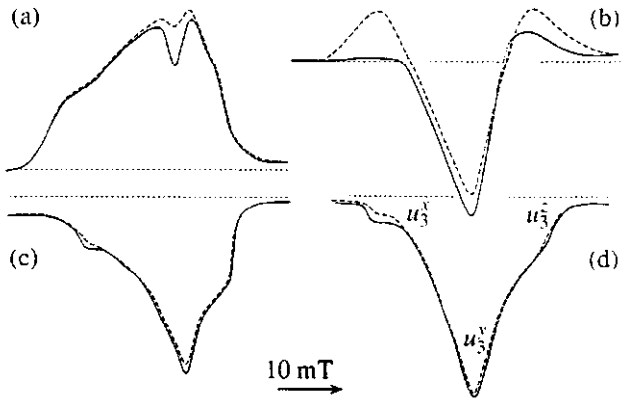

Fig. 3. First-derivative 2-mm waveband EPR dispersion spectra showing (a, b) in-phase and (c, d) quadrature components for the (a, c) initial and (b, d) doped PTTF samples measured at room temperature (solid curves) and 160 K (dashed curves).

$\omega_m T_1 > 1$ and $\omega_m T_1 < 1$, respectively, the total signal of dispersion from these samples will be determined primarily by the terms u_2, u_3 and u_1, u_3 of equation (3), respectively (Fig. 3). Note that the main components of the quadrature component of the dispersion signal are detected at somewhat higher magnetic field strengths

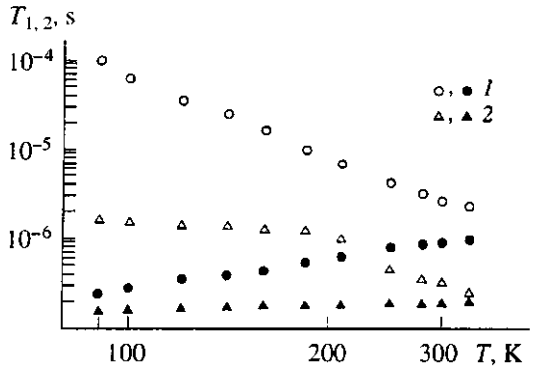

Fig. 4. Logarithmic plots of the spin–lattice (T_1, open symbols) and spin–spin (T_2, black symbols) relaxation times of the paramagnetic centers in the (*1*) initial and (*2*) doped PTTF.

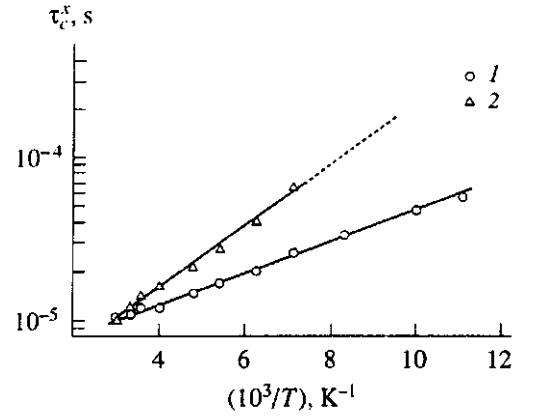

Fig. 5. Arrhenius plots of the correlation time τ_c^x of the anisotropic libration of polymer chains in the (*1*) initial and (2) doped PTTF.

(g_{xx}^d = 2.01188, g_{yy}^d = 2.00571, and g_{zz}^d = 2.00231 (Figs. 3c and 3d) as compared to the corresponding inphase components of the absorption and dispersion signals.

The relaxation times for the paramagnetic centers of both types can be determined from analysis of the dispersion signal components u_i measured using a specially adjusted phase detector as described in [26]. Figure 4 shows the temperature variation of the parameters T_1 and T_2 of the samples studied. As can be readily checked, the value of T_1 in PTTF-1 varies with the temperature by the law $T \propto T^{-3.0}$. This behavior is not consistent with the Raman relaxation interaction between spin and harmonic lattice vibrations, which involves the absorption of two phonons and obeys the relationship $T \propto T^{-2}$ for $T > 20$ K [27]. At the same time, the T_2 value of the same sample exhibits a nearly linear variation with the temperature. The spin–spin relaxation time in the doped samples depends on the temperature to a much lesser extent (Fig. 4). A weak temperature dependence is also characteristic of the spin–lattice relaxation time in the range 90–200 K, although at higher temperatures this quantity varies by the law $T_1 \propto T^{-2.1}$.

As is seen from the spectra presented in Figs. 3c and 3d, the shape of the quadrature component of the dispersion signal in the samples studied is temperature-dependent. As was demonstrated previously [11, 18], this change in the shape of the EPR spectrum is caused by the SHF saturation transfer effects (ST-EPR) [28] related to the superslow (correlation times above 0.1 s) libration (torsional) motions of the polymer chains containing localized paramagnetic centers.

The ratio u_3^x/u_3^y (which is the most sensitive with respect to these motions) increases with the temperature (Fig. 3c and 3d). This can be related to a superslow anisotropic reorientation of the polymer chains (with localized paramagnetic centers acting as natural sensitive labels) relative to the crystallographic *c*-axis. Using the method described in [11], we have determined the correlation times τ_c^x of these librations from the results of 2-mm waveband ST-EPR measurements. These parameters are equal to $5.2 \times 10^{-6}\exp(0.019\ \text{eV}/k_BT)$ and $2.4 \times 10^{-6}\exp(0.04\ \text{eV}/k_BT)$ (k_B is the Boltzmann constant) for the initial and doped PTTF samples, respectively (Fig. 5). The experimental results obtained indicate that superslow anisotropic motions in the doped PTTF samples appear at higher temperatures and have greater activation energies (as compared to the initial samples), which is probably explained by higher rigidity of the doped polymer. An analysis of the ST-EPR spectra showed that the quadrature components of the dispersion signal in both initial and doped PTTF samples are sensitive to the libration oscillations beginning with 100 and 130 K, respectively. From these results we may estimate the maximum correlation time registered in the 2-mm waveband EPR spectra of the samples studied in this work as $\tau_c^{max} \approx 10^{-4}$ s, which is close to the analogous value for PTTF with monomer units linked by phenyl bridges [14].

For interpretation of the relaxation parameters of the paramagnetic centers in PTTF, we have suggested that polarons in PTTF (as well as those in other polymeric semiconductors [11–13]) are capable of diffusing along the macromolecular chain and hopping between chains at the rates $\nu_{1D} > \nu_{1D}^0$ and ν_{3D}, respectively. This mobility is characterized by the spectral density function [29]

$$J(\omega) = n\phi(\omega)\Sigma_{ij}, \qquad (4)$$

where $n = (n_1 + n_2)/\sqrt{2}$ is the effective concentration (per PTTF monomer unit) of localized (n_1) and delocalized (n_2) paramagnetic centers, Σ_{ij} is the lattice sum for

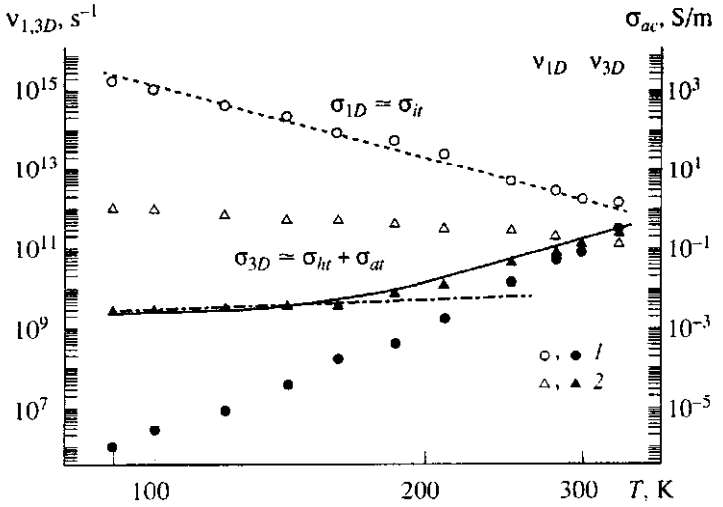

Fig. 6. Experimental logarithmic temperature dependences of the rates of intrachain (ν_{1D}, open symbols) and interchain (ν_{3D}, black symbols) diffusion of polarons in the (*1*) initial and (*2*) doped PTTF. The curves show high-frequency ac conductivities calculated by the equations $\sigma_{1D} = 4.2 \times 10^{-13}\nu_e T^{-1}[\ln(1.9 \times 10^{28}\nu_e T^{14.2})]^4$ [equation (8b), dashed line], $\sigma_{3D} = 4.2 \times 10^{-19}\nu_e T[\ln(4 \times 10^{12}\nu_e^{-1})]^4$ [equation (10b), dash-dot line], and $\sigma_{3D} = 4.2 \times 10^{-19}\nu_e T[\ln(4 \times 10^{12}\nu_e^{-1})]^4 + 2.3 \times 10^{-12}\nu_e^{0.8} T\exp(-0.045\ \text{eV}/k_B T)$ [equations (10b) and (11b), solid line].

the powdered PTTF sample, ω is the working frequency, and

$$J_{1D}(\omega) = \frac{1}{\sqrt{4\pi\nu_{1D}\nu_{3D}}}\sqrt{\frac{1+\sqrt{1+(\omega/\nu_{3D})^2}}{1+(\omega/\nu_{3D})^2}}$$

$$= \begin{cases} (2\nu_{1D}\omega)^{-1/2} & \text{at} \quad \nu_{1D} \gg \omega \gg \nu_{3D} \\ (4\pi\nu_{1D}\nu_{3D})^{-1/2} & \text{at} \quad \omega \ll \nu_{3D}. \end{cases}$$

Taking into account that the electron relaxation is determined primarily by the dipole–dipole interaction between localized and delocalized spins, we may write the following equations for the electron relaxation rates [30]:

$$T_1^{-1} = \langle\omega^2\rangle[2J(\omega) + 8J(2\omega)] \qquad (5a)$$

$$T_2^{-1} = \langle\omega^2\rangle[3J(0) + 5J(\omega) + 2J(2\omega)], \qquad (5b)$$

where $\langle\omega^2\rangle = 0.1(\mu_0/4\pi)^2\gamma_e^4\hbar^2 S(S+1)n\Sigma_{ij}$ is the averaged spin interaction constant for the powder, μ_0 is the permeability of vacuum, and S is the spin of the paramagnetic center.

Figure 6 shows the temperature variation of the frequencies ν_{1D} and ν_{3D} calculated by equations (5) using the data of Fig. 4 for an average polaron length of 5 monomer units [31]. As is seen from this figure, $\nu_{1D} = 1.4 \times 10^{12}$ and 1.3×10^{11} s^{-1} for the initial and doped samples at room temperature. These values markedly exceed the rate of one-dimensional (*1D*) diffusion of polarons in PTTF with monomer units linked by phenyl bridges [14], which is probably explained by a more planar conformation of the samples studied in this work. Indeed, upon going from PTTF with monomer units linked by phenyl bridges to the polymer with TTF units linked by tetrahydroanthracene, the quantity g_{xx} (the most sensitive to changes in the macromolecular conformation) decreases from 2.01424 [14] to 2.01292, that is, by $\Delta g = 1.32 \times 10^{-3}$. The integral I_{ij} of overlap between the π-orbitals of the neighboring TTF groups (like that in the other conjugated polymers and hydrocarbons [32]) depends on the dihedral angle θ (i.e., the angle between the planes of the TTF groups) according to the cosine law $I_{ij} \propto \cos\theta$ [33]. Therefore, we may determine a change in the dihedral angle using the following modified equation [34]:

$$\Delta g_{xx} = \frac{2\lambda_S\rho_S^0(1 + k_1\sin\theta)}{\Delta E_{ex}(1 - k_2\cos\theta)}, \qquad (6)$$

where λ_S is the constant of spin–orbit coupling between the spin and sulfur atom, ρ_S^0 is the spin density on sulfur atom, ΔE_{ex} is the minimum electron excitation energy, and k_1, k_2 are constants. According to this formula, a change in the dihedral angle upon going from PTTF with monomer units linked by phenyl bridges to the polymer having a more planar configuration with TTF units linked by tetrahydroanthracene was $\Delta\theta = 22°$. This value is close, for example, to $\Delta\theta = 23°$

observed upon going from benzoid to quinoid form of poly(phenylene) [6] or from initial (unoxidized) to oxidized poly(aniline) [33, 35].

The conducting properties of the organic semiconductors studied can be studied within the framework of different theoretical models. Let us write the conductivity equation for PTTF in the most general form:

$$\sigma = \sigma_{it} + \sigma_{at} + \sigma_{ht}, \quad (7)$$

where σ_{it}, σ_{at}, and σ_{ht} denote contributions of the isoenergetic, activation, and hopping tunneling charge transfer modes, respectively.

In a neutral polymer, the dominating process consists in a quasi-one-dimensional charge transfer by nonlinear excitations along individual polymer chains. This transfer mode is most adequately described by a phenomenological model of Kivelson [36] based on the resonance dimerization of *trans*-poly(acetylene) modulated by the interaction of charge carriers with optical lattice phonons, which was successfully used for description of the electron transport in low-conductivity *trans*-poly(acetylene) [5]. Kivelson [37] suggested that modulation of this type is also possible in other conducting polymers where the charge is transferred between soliton-like polaron–bipolaron pairs. This hypothesis was confirmed by the results of investigations of the charge transfer in low-doped poly(phenylene) [38] and poly(aniline) [35, 39]. According to the modified Kivelson model, localization of a charge carrier near a counterion allows the charge to tunnel between the nonlinear carriers at a rate of $\gamma(T) \propto T^{m+1}$ ($m \approx 10$ for a spin interacting with the optical lattice phonons) with a sufficiently low activation energy. Taking into account that PTTF, unlike *trans*-poly(acetylene), has charged polarons and bipolarons, the Kivelson equations for the dc and ac conductivity [36] should be modified and written in the following form [38]:

$$\sigma_{dc}(T) = \frac{k_1 e^2 \gamma(T) \xi \langle y \rangle}{k_B T N_i R_0^2} \exp\left(\frac{2k_2 R_0}{\xi}\right) = \sigma_0 T^m \quad (8a)$$

$$\sigma_{ac}(T) = \frac{N_i^2 e^2 \langle y \rangle \xi_{\parallel}^3 \xi_{\perp}^2 \nu_e}{384 k_B T} \left[\ln \frac{2\nu_e}{\langle y \rangle \gamma(T)}\right]^4 = \frac{\sigma_0 \nu_e}{T} \left[\ln \frac{k_3 \nu_e}{T^{m+1}}\right]^4. \quad (8b)$$

where $k_1 = 0.45$, $k_2 = 1.39$, and k_3 are constants; $\gamma(T) = \gamma_0 (T/300\ \mathrm{K})^{m+1}$ is the rate of charge transfer between polaron and bipolaron; $\langle y \rangle = y_p y_{bp} (y_p + y_{bp})^{-2}$, y_p and y_{bp} being the numbers of polarons and bipolarons per monomer unit, respectively; $R_0 = (4\pi N_i/3)^{-1/3}$ is the average distance between dopant molecules, N_i is the dopant concentration, $\xi = (\xi_{\parallel} \xi_{\perp}^2)^{1/3}$, $\xi_{\parallel}$ and $\xi_{\perp}$ are the space-average, parallel, and perpendicular components of the charge carrier wavefunction, and $\nu_e = \omega_e/2\pi$.

Assuming the value $k_3 = 90.8$ for the initial PTTF sample and substituting the slope of the $\nu_{1D}(T)$ plot into equation (8b), we obtain for this polymer $m = 13.2$ and $y_{bp} = 7.5 \times 10^{-5}$. The conductivity can be calculated using the formula

$$\sigma_{1,3D} = N e^2 \nu_{1,3D} c_{1,3D}^2 / k_B T, \quad (9)$$

where N is the volume concentration of charge carriers and c is the lattice constant. For $N = 2 \times 10^{23}$ m^{-3} and $c_{1D} = 1.2$ nm, the data plotted in Fig. 6 provide a room-temperature conductivity estimate of $\sigma_{1D} = 1.8$ S/m. Adopting the values $\xi_{\parallel} = 6$ nm, $\xi_{\perp} = 0.6$ nm, $y_p = 4.3 \times 10^{-4}$, $\langle y \rangle = 0.11$, and $\sigma_{dc} = 4.2 \times 10^{-5}$ S/m ($T = 300$ K) [10], we may calculate by equations (8) that $\gamma(T) = 1.3 \times 10^{-25} T^{14.2}$ s^{-1}, $N_i = 3.3 \times 10^{24}$ m^{-3}, and $R_0 = 4.2$ nm.

Figure 6 also presents the curve $\sigma_{1D}(T)$ calculated for the initial PTTF sample by equation (8b), which is seen to provide a good approximation for the function $\nu_{1D}(T)$. The ratio $\sigma_{ac}/\sigma_{dc} = 4 \times 10^4$ obtained for this sample from equations (8) is close to the value reported for *trans*-poly(acetylene) [5].

As is seen from Fig. 6, the polaron diffusion rate in a doped PTTF sample can be approximated by a linear function in the low- temperature region and varies more rapidly at temperatures above 150 K. This behavior reflects a weak spin–phonon coupling in the doped samples at low temperatures, which is a typical feature of the semiconductor systems of higher dimensionality and agrees with the data reported previously for the conductivity in PTTF [10, 40]. Therefore, we may conclude that a dominating mechanism of the charge transfer in these systems is the variable-range 3*D*-hopping charge transfer described within the framework of the Mott theory [41]. In equation (7), the term σ_{ht} contains two contributions

$$\sigma_{dc} = 0.39 \nu_0 e^2 \sqrt{\frac{n(\varepsilon_F) L}{k_B T}} \exp[-(T_0/T)^{1/4}] \quad (10a)$$

$$\sigma_{ac} = \frac{2}{3} \pi^2 e^2 k_B T n^2(\varepsilon_F) L^5 \nu_e (\ln \nu_0 / 2\pi \nu_e)^4, \quad (10b)$$

where ν_0 is the hopping frequency limit, $T_0^{-1} = 6.3 \times 10^{-2} k_B n(\varepsilon_F) L^3$ is the percolation parameter for the given compound, $n(\varepsilon_F)$ is the density of states at the Fermi level, and L is the average range of the electron wavefunction. Extrapolation of the $\nu_{3D}(T)$ plot from the low-temperature region to higher temperatures yields $\nu_{3D}(T) = 4.8 \times 10^9$ s^{-1} and $\sigma_{dc} = 7.2 \times 10^{-6}$ S/m at 300 K. Adopting $\xi = L$ and $\nu_0 = 2.5 \times 10^{13}$ s^{-1} for PTTF with monomer units linked by phenyl bridges [14], we obtain,

using equations (10), that $n(\varepsilon_F) = 1.1 \times 10^{24}$ eV^{-1} m^{-3} and $T_0 = 7.8 \times 10^7$ K.

An analysis of the high-temperature part of the $\nu_{3D}(T)$ dependence shows that the interchain conductivity at $T > 160$ K is determined predominantly by the terms σ_{ht} and σ_{at} in equation (7). As is seen from Fig. 6, the activation process increases the conductivity of PTTF samples at 300 K by more than one order of magnitude. The conductivity σ_{ht} calculated by equation (10b) is 0.018 S/m. Substituting this value into equation (9), we obtain an estimate for a total concentration of the nonlinear charge carriers $N = N_p + N_{bp} = 4.5 \times 10^{23}$ m^{-3}, which is close to the total concentration of paramagnetic charge carriers in PTTF-2 and PTTF-3. Using equations (10), we obtain that the ac/dc conductivity ratio $\sigma_{ac}(\nu_e \longrightarrow \infty)/\sigma_{dc} = 108(T/T_0)^{1.5}\exp[(T/T_0)^{0.25}] = 5220$ for PTTF-3. This yields $\sigma_{ht} + \sigma_{at} = 4.4 \times 10^{-5}$ S/m, which is close to $\sigma_{dc} = 1.5 \times 10^{-4}$ S/m reported for PTTF-3 at 300 K [10].

In PTTF, the term σ_{at} in equation (7) is determined for the most part by activation (with the energy E_a) of the charge carriers from localized energy levels in the forbidden band [42]:

$$\sigma_{dc} = \sigma_0 \exp(-E_a/k_B T) \tag{11a}$$

$$\sigma_{ac} = \sigma_0 \nu_e^s T \exp(-E_a/k_B T), \tag{11b}$$

where s is a characteristic parameter. As can be seen from Fig. 6, the high-temperature branch of the $\nu_{3D}(T)$ dependence is rather well approximated by the superposition of the functions (10b) and (11b) with $E_a = 0.045$ eV. This is evidence of a close relationship between the charge-transfer and macromolecular dynamics in PTTF. It must be noted that this activation energy is close to the values for the superslow librations of PTTF chains with monomer units linked by phenyl bridges [14] for the PTTF-2 and PTTF-3 samples studied in this work (see above), and for polyacenes [43], but is lower as compared to $E_a = 0.045$ eV reported for poly(aniline) [35, 39].

Madhukar [44] demonstrated that fluctuations of the lattice oscillations (e.g., librations) in systems of lower dimensionality can modulate the energy of charges localized at the lattice sites and the integral I_{ij} of the interchain charge transfer. A similar situation apparently takes place in PTTF samples where the libron oscillations of macromolecular segments can modulate the I_{ij} integral, thus inducing incoherent interchain charge transfer with $E_a \equiv 0.04$ eV corresponding to the energy of optical phonons. Because the polymer chains in PTTF with monomer units linked by phenyl bridges possess a greater degree of freedom than the chains in PTTF-2 and PTTF-3 samples, this modulation mode is effective in the former polymer at lower temperatures [14], where the term σ_{at} in equation (7) makes the dominant contribution to the total conductivity.

Within the framework of the model of charge transfer via a nontransparent interchain energy barrier, the mobility of charge carriers must significantly depend on the barrier height, the latter rapidly increasing with E_a. The conjugation range and, hence, the number of π-electrons in the samples studied in this work are somewhat lower compared to those in PTTF with monomer units linked by phenyl bridges. This may result in a higher transfer activation energy and mobility of charge carriers in PTTF-2 and PTTF-3, similarly to what was observed in some other π-conjugated systems [45, 46]. Substitution of tetrahydroanthracene bridges for the phenyl ones leads to an increase in the mobility, not accompanied by any significant change in the activation energy, probably, because of a compensation effect. The compensation may result from a combined effect of three factors, including increased chain planarity in PTTF monomer units linked by tetrahydroanthracene bridges, reduced effective E_a, and increased transfer integral between π-orbitals of monomer units, leading to a higher rate of both intra- ad interchain charge transfer.

The libron–exciton interactions arising in the doped PTTF are indicative of the formation of a complex quasi-particle, namely, the molecular-lattice polaron. Within the framework of this phenomenological model under consideration, it is possible to assume that the molecular polaron, possessing mobility of the type $\mu_m \propto T$, is involved in an additional lattice polarization. Because the mobility of a lattice polaron has the activation character, the resulting mobility of the quasi-particle will consist of the contributions due to mobilities of the molecular (μ_m) and lattice (μ_l) polarons:

$$\begin{aligned}\mu_{ml}(T) &= \mu_m(T) + \mu_l(T) \\ &= aT + b\exp(-E_a/k_B T),\end{aligned} \tag{12}$$

where a and b are constants. The energy of the lattice polaron binding in PTTF can be estimated as $E_{pl} = 2E_a = 0.07$–0.08 eV, which is close to the order of magnitude to the energy of formation of such a quasi-particle in crystalline naphthalene [47].

As is seen from Fig. 6, the characteristic times of charge carrier hopping between chain sites and between adjacent macromolecules in PTTF-1 at room temperature are $\tau_h^{\parallel} = \nu_{1D}^{-1} = 4 \times 10^{-13}$ s and $\tau_h^{-} = \nu_{3D}^{-1} = 7.7 \times 10^{-12}$ s. The introduction of dopant and the increase in dimensionality render these times approximately equal, and they acquire a room-temperature value of approximately $\tau_h = \tau_h^{\parallel} \equiv \tau_h^{\perp} = 8 \times 10^{-12}$ s. Therefore, the corresponding transfer integrals determined from the Heisenberg relationship $I_{ij} = \hbar/\tau_h$ are $I_{ij}^{\parallel} = 1.6 \times 10^{-3}$ eV, $I_{ij}^{\perp} = 8.6 \times 10^{-5}$ eV for PTTF-1 and

$I_{ij}^{\parallel} \equiv I_{ij}^{\perp} = 1 \times 10^{-4}$ eV for PTTF-2 and PTTF-3. Assuming that the energies of polaron formation in PTTF and polyacene crystals have close values $E_{pm} = 0.15$ eV [48], the energy of the molecular-lattice polaron formation in PTTF can be estimated as $E_{pml} = E_{pm} + E_{pl} \approx 0.19$ eV. Therefore, a minimum time necessary for the polarization of atomic and molecular orbitals in the polymer is $\tau_e = \hbar / E_{pml} = 3.5 \times 10^{-15}$ s. From this it follows that the period of charge carrier hopping in PTTF is longer by 2–3 orders of magnitude as compared to the time required for the electron subsystem polarization in macromolecules surrounding a delocalized charge carrier: $\tau_h \gg \tau_e$. This inequality determines the necessary and sufficient condition for the electron polarization of polymer chains by the charge carrier and serves a criterion for the need of taking into account the electron polarization in studying the charge carrier dynamics and determining the energy structure of a polymer semiconductor.

Upon inelastic scattering of an electron possessing the effective mass m_e and the Fermi velocity v_F, the electron will have an excess energy of $E_k = m_e v_F^2/2$. Taking into account that the process has a two-phonon mechanism and the energy of optical phonons is $2h\nu_{ph} = E_k = 0.21$ eV at $\nu_{ph} = 2.5 \times 10^{13}$ s^{-1} [14], we obtain an estimate of the Fermi velocity $v_F = 1.9 \times 10^5$ m/s. Using this value, we may also estimate the free range of charge carriers by the formula $l^* = \nu_{1D} c_{1D}^2 v_F^{-1}$, which yields $l^* = 2 \times 10^{-2}$ nm for PTTF-1 and 2×10^{-3} nm for PTTF-2 and PTTF-3. These values are too small to consider PTTF chains (with monomer units linked by tetrahydroanthracene bridges) as a quasi-metal.

CONCLUSIONS

The data obtained in this work indicate that a dominating conductivity mechanism in the initial (undoped) PTTF is the isoenergetic anisotropic tunneling of charge carriers that can be described within the framework of the Kivelson formalism. The probability of this process is determined by a quasi-one-dimensional polaron dynamics, which depends on the structure and conformation of polymer chains. The introduction of dopant increases the conductivity of PTTF by almost 2 orders of magnitude without any significant growth in the concentration of paramagnetic centers. This can be explained by activation ("defreezing") of the one-dimensional mobility of polarons, followed by their partial collapse with the formation of diamagnetic bipolarons.

The charge transfer at low temperatures in the doped PTTF with monomer units linked by tetrahydroanthracene bridges, which has a more planar chain conformation than the undoped polymer, proceeds by mechanism of the variable-range hopping of charge carriers. Upon heating above the critical point (about 160 K), the total number of lattice phonons exhibits a sharp growth and the lattice oscillations involve a large number of different modes. This results in stronger interaction of a part of excitons with the phonon field. Because the transfer integral I_{ij} is an exponential function of the polymer chain separation, a higher energy of the lattice oscillations leads to an increase in the effective I_{ij} value. As a result, the "statistical" potential barriers involved in the classical Mott theory are replaced by the "dynamic" barriers, with the probability of penetration through these barriers modulated by macromolecular oscillations.

ACKNOWLEDGMENTS

The authors are grateful to S.D. Chemerisov and I.B. Nazarova for their help in conducting experiments.

REFERENCES

1. *Electronic Properties of Polymer*, Kuzmany, H., Mehring, M., and Roth, S., Eds., Berlin: Springer, 1992.
2. *Polyconjugated Materials*, Zerbi, G., Ed., Amsterdam: Norht-Holland, 1992.
3. *Proc. Int. Conf Science, and Technology of Synthetic Metals (ICSM'96)*, Snowbird, USA (1996), *Synth. Met.*, 1997, vol. 84.
4. Chien, J.C.W., *Polyacetylene: Chemistry, Physics and Material Science*, Orlando: Academic, 1984.
5. Epstein, A.J., *Handbook of Conducting Polymers*, Skotheim, T.A., Ed., New York: Marcel Dekker, 1986, vol. 2, p. 1041.
6. Brédas, J.-L., *Handbook of Conducting Polymers*, Skotheim, T.A., Ed., New York: Marcel Dekker, 1986, vol. 2, p. 859.
7. Bernier, F., *Handbook of Conducting Polymers*, Skotheim, T.A., Ed., New York: Marcel Dekker, 1986, vol. 2, p. 1099.
8. Mizoguchi, K., *Makromol. Chem., Macromol. Symp.*, 1990, vol. 37, p. 53.
9. Roth, H.-K., Gruber, H., Fanghänel, E., and Trinh Vu Quang, *Prog. Colloid. Polym. Sci.*, 1988, vol. 78, p. 75.
10. Roth, H.-K., Brunner, W., Volkel, G., Schrödner, M., and Gruber, H., *Makromol. Chem., Macromol. Symp.*, 1990, vol. 34, p. 293.
11. Krinichnyi, V.I., *2-mm Wave Band EPR Spectroscopy of Condensed Systems*, Boca Raton: CRC, 1995.
12. Krinichnyi, V.I., *Usp. Khim.*, 1996, vol. 65, no. 1, p. 84.
13. Krinichnyi, V.I., *Usp. Khim.*, 1996, vol. 65, no. 6, p. 564.
14. Krinichnyi, V.I., Pelekh, A.E., Roth, H.-K., and Lüders, K., *Appl. Magn. Reson.*, 1993, vol. 4, p. 345.
15. Roth, H.-K. and Krinichnyi, V.I., *Makromol. Chem., Macromol. Symp.*, 1993, vol. 72, p. 143.
16. Le van Hinh Schukat, G. and Fanghänel, E., *J. Prakt. Chem.*, 1979, vol. 321, p. 299.
17. Galkin, A.A., Grinberg, O.Ya., Dubinskii, A.A., Kabdin, N.I., Krymov, V.N., Kurochkin, V.I., Lebedev, Ya.S., Oranskii, L.G., and Shuvalov, V.F., *Prib. Tekh. Eksp.*, 1977, vol. 4, p. 284.

18. Krinichnyi, V.I., *Appl. Magn. Reson.*, 1991, vol. 2, p. 29.
19. Blyumenfel'd, L.A., Voevodskii, V.V., and Semenov, A.G., *Primenenie Elektronnogo Paramagnitnogo Rezonansa v Khimii* (Application of Electron Paramagnetic Resonance in Chemistry), Novosibirsk: Akad. Nauk SSSR, 1962.
20. Bolton, J.R., *Mol. Phys.*, 1963, vol. 6, p. 219.
21. Fitzky, H.G. and Hocker, J., *Synth. Met.*, 1986, vol. 13, p. 335.
22. Pool, Ch.P., *Electron Spin Resonance: a Comprehensive Treasure on Experimental Techniques*, New York: Wiley, 1983, p. 440.
23. Al'tshuler, S.A. and Kozyrev, B.M., *Elektronnyi Paramagnitnyi Rezonans Soedinenii Promezhutochnykh Grupp* (Electron Paramagnetic Resonance of the Compounds of Intermediate Groups), Moscow: Nauka, 1972.
24. Carrington, A. and McLachlan, A.D., *Introduction to Magnetic Resonance with Application to Chemistry and Chemical Physics*, New York: Harper, 1967.
25. Gullis, P.R., *J. Magn. Reson.*, 1976, vol. 21, p. 397.
26. Pelekh, A.E., Krinichnyi, V.I., Brezgunov, A.Yu., Tkachenko, L.I., and Kozub, G.I., *Vysokomol. Soedin., Ser. A*, 1991, vol. 33, no. 8, p. 1731.
27. Kurzin, S.P., Tarasov, B.G., Fatkulin, N.F., and Aseeva, R., *Vysokomol. Soedin., Ser. A*, 1982, vol. 24, no. 1, p. 117.
28. Hyde, J.S. and Dalton, L., *Spin Labeling. Theory and Application*, London: Academic, 1979, vol. 2, p. 1.
29. Butler, M.A., Walker, L.R., and Soos, Z.G., *J. Chem. Phys.*, 1976, vol. 64, p. 3592.
30. Abraham, A., *The Principles of Nuclear Magnetism*, Oxford: Oxford Univ., 1961.
31. Devreux, F., Genoud, F., Nechtschein, M., and Villeret, B., *Electronic Properties of Conjugated Polymers*, Kuzmany, H., Mehring, M., and Roth, S., Eds., Berlin: Springer, 1987.
32. Traven', V.F., *Elektronnaya struktura i svoistva organicheskikh molekul* (Electron Structure and Properties of Organic Molecules), Moscow: Khimiya, 1989.
33. Masters, J.G., Ginder, J.M., MacDiarmid, A.G., and Epstein, A.J., *J. Chem. Phys.*, 1992, vol. 96, p. 4768.
34. Buchachenko, A.L. and Vasserman, A.M., *Stabil'nye radikaly* (Stable Radicals), Moscow: Khimiya, 1973.
35. Krinichnyi, V.I., Chemerisov, S.D., and Lebedev, Ya.S., *Phys. Rev. B: Condens. Matter*, 1997, vol. 55, p. 16233.
36. Kivelson, S., *Phys. Rev. B: Condens. Matter*, 1982, vol. 25, p. 3798.
37. Kivelson, S., *Mol. Cryst. Liq. Cryst.*, 1981, vol. 77, p. 65.
38. Kuivalainen, P., Stubb, H., Isotalo, H., Yli-Lahti, P., and Holmström, C., *Phys. Rev. B: Condens. Matter*, 1985, vol. 31, p. 7900.
39. Krinichnyi, V.I., Chemerisov, S.D., and Lebedev, Ya.S., *Synth. Met.*, 1997, vol. 84, p. 819.
40. Gruber, H., Roth, H.-K., Patzsch, J., and Fanghänel, E., *Makromol. Chem., Macromol. Symp.*, 1990, vol. 37, p. 99.
41. Mott, N. and Davis, E., *Electronic Processes in Non-Crystalline Materials*, Oxford: Oxford Univ. Press, 1979.
42. Patzsch, J. and Gruber, H., *Electronic Properties of Polymers*, Kuzmany, H., Mehring, M., and Roth, S., Eds., Berlin: Springer, 1992, vol. 107, p. 121.
43. Silinsh, E.A., *Organic Molecular Crystals. Their Electronic States*, Heidelberg: Springer, 1980, vol. 16.
44. Madhukar, A. and Post, W., *Phys. Rev. Lett.*, 1977, vol. 39, p. 1424.
45. Eley, D.D. and Parfitt, G.D., *Trans. Faraday Soc.*, 1955, vol. 51, p. 1529.
46. Many, A., Harnik, E., and Gerlick, D., *J. Chem. Phys.*, 1955, vol. 23, p. 1733.
47. Carl, N., *Proc. XI Symp. On Molecular Crystals*, Lugano, Switzerland, 1985, p. 135.
48. Silin'sh, E.A., Kurik, M.V., and Chapek, V., *Elektronnye protsessy v organicheskikh molekulyarnykh kristallakh: yavleniya lokalizatsii i polyarizatsii* (Electron Processes in Organic Molecular Crystals: Localization and Polarization Phenomena), Riga: Zinatne, 1988.